

Identification of the Active EPA/AA-Binding Ether-Type Phosphatidylcholine Derived from the Starfish *Patiria pectinifera* for C2C12 Myotube Growth

Aoi Fukushima, Kyosuke Imamura, Naoki Takatani, Masashi Hosokawa, and Fumiaki Beppu*



Cite This: *ACS Omega* 2024, 9, 45564–45571



Read Online

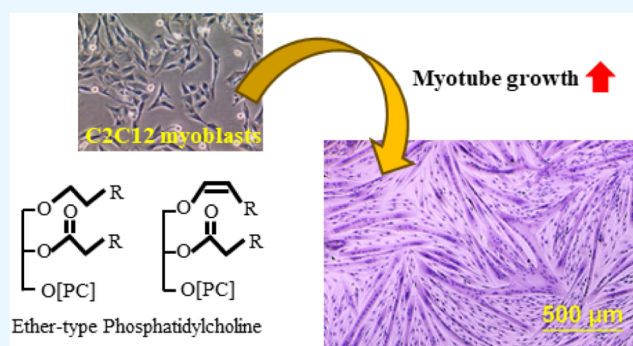
ACCESS |

Metrics & More

Article Recommendations

Supporting Information

ABSTRACT: Concerns about nutritional approaches for promoting skeletal muscle mass and function have increased. This study assessed the effects of starfish-derived glycerophospholipids (PLs) (SPL), characterized by unique ether-linked subclasses, alkylacyl (Alk)- and alkenylacyl (Pls)-PL, on skeletal muscle function, focusing on myotube formation in C2C12 myoblasts. SPL was prepared via chloroform/methanol extraction from *Patiria pectinifera*, followed by silica gel chromatography fractionation. Myoblasts were induced to differentiate with or without SPL treatment. On day 7 of differentiation, 50 $\mu\text{g}/\text{mL}$ of SPL treatment increased myotube diameter. The phosphatidylcholine (PC) fraction (SPC) also enhanced myotube growth at 30 $\mu\text{g}/\text{mL}$. LC-MS/MS analysis indicated the most abundant PC molecular species in SPC were Alk- and Pls-PC with eicosapentaenoic acid and arachidonic acid. Treatment with 1-*O*-hexadecyl-2-arachidonoyl-PC, 1-1(*Z*)-hexadecenyl-2-arachidonoyl-PC or 1-*O*-hexadecyl-2-eicosapentaenoyl-PC increased myotube diameter and myokine Il-15 mRNA expression. These results demonstrate a novel functionality of SPC and highlight the role of ether-type PC molecules in muscle function.



INTRODUCTION

The loss of muscle mass and weakness are recognized as risk factors for fragility and mortality.^{1–3} Skeletal muscle is critical for physical activity, exercise, and energy metabolism. Its reduction not only decreases physical activity but also leads to obesity-related metabolic disorders due to metabolic inactivity.^{4,5} Promoting and maintaining skeletal muscle mass and function is a global health priority, particularly in countries with aging populations. However, medical treatments to reverse skeletal muscle atrophy caused by aging and lack of exercise are not well established. To address these issues in the growing older population, nutritional approaches involving functional food factors are of great interest.^{6,7}

Glycerophospholipids (PLs) are essential components of biological membranes in terrestrial and marine organisms and are one of the most nutritionally important lipid compounds. Marine-derived PLs, rich in *n*-3 polyunsaturated fatty acids (*n*-3PUFA), such as eicosapentaenoic acid (EPA) and docosahexaenoic acid (DHA), have been attracted attention for their health benefits, including the improvement of metabolic disorders, due to their high bioavailability and incorporation into tissues and cells.^{8–10} PUFA-PLs play a crucial role in regulating membrane fluidity, membrane protein function, and cell signaling. *In vitro* experiments have shown that PUFA-PLs are biologically active in modulating cell proliferation and

differentiation.^{11,12} PLs include ether-type subclasses, such as alkylacyl-PLs (Alk-PLs) and plasmalogen-PLs (Pls-PLs), where the alkyl/alkenyl chain is bound by an ether linkage at the *sn*-1 position of the glycerol backbone, as opposed to the more common diacyl-type PLs. Ether-PLs are vital in maintaining cell membrane homeostasis and stability, contributing to antioxidant activity and signal transduction.¹³ Interestingly, *in vivo* studies using ether-PLs derived from marine organisms have shown intestinal absorption¹⁴ and functional efficiencies, such as a preventive effect against atherosclerosis¹⁵ and fatty liver disease.¹⁶ However, only few studies have focused on the differences in functionality due to the ether-bond structure, and the physiological functions of ether-PLs in skeletal muscles remain unclear.

In the present study, we prepared ether PL-rich starfish-derived PL (SPL) and aimed to identify its effect on muscle function, with a specific focus on myotube formation in C2C12 mouse myoblast cells. Starfish have been paid attention on a

Received: August 26, 2024

Revised: October 12, 2024

Accepted: October 23, 2024

Published: October 30, 2024



valuable research source of many bioactive lipid compounds, including steroids, steroidal glycosides, glycosphingolipids, terpenoids, and carotenoids.^{17,18} In addition, various starfish species are commonly rich in Alk-PL and Pls-PL.¹⁹ Diverse biologically active lipid compounds from echinoderms, including starfish, have demonstrated anticancer, anti-inflammatory, and neurotogenic activities, as well as improvements in metabolic disorders.^{17,20–22} However, no studies have investigated the effect of these compounds on skeletal muscle function. In the present study, we found that SPL and its phosphatidylcholine (PC) fraction (SPC) promote myotube growth and identified the PUFA-binding ether-PC molecules as the active compound. In the discussion, we shall present differences in myotube growth among PC subclasses in skeletal muscle cells. These findings highlight the novel functional properties of ether-PL and -PC molecules in myotube growth and function.

RESULTS

Effects of SPL on Myotube Formation in C2C12 Cells.

Silica gel chromatography resulted in the isolation of three fractions mainly composed of neutral lipids, glycolipids, and SPL, with respective compositions of $41.4 \pm 4.9\%$, $17.0 \pm 2.6\%$, and $41.6 \pm 3.9\%$ (wt %), respectively. We then assessed the effects of SPL on myotube formation in C2C12 myoblast cells by exposing them to $50 \mu\text{g/mL}$ of SPL during differentiation. Notably, SPL treatment enhanced myotube growth, as evidenced by an increase in myotube diameter on day 7 (Figure 1a). When measuring the diameters of 50 myotubes in each well, the most abundant diameters in control cells were 10–15 μm and 15–20 μm . However, SPL treatment significantly increased the proportion of large-sized myotubes with diameters greater than 25 μm (Figure 1b). Furthermore, SPL treatment elevated the mRNA expression levels of myogenic genes, such as MyoD, myogenin, and myokine IL-15 (Figure 1c).

Effects of SPC on Myotube Formation in C2C12 Cells.

Preparative TLC analysis revealed that SPL contained a high abundance of PC, accounting for more than 45% (w/w) (PC: $45.8 \pm 5.1\%$, phosphatidylethanolamine (PE): $29.4 \pm 2.7\%$, phosphatidylserine (PS): $14.8 \pm 4.3\%$, lysophosphatidylcholine (LPC): $10.0 \pm 2.3\%$ (w/w)). Therefore, we focused on the SPC fraction in this study. Immunostaining with anti-MyHC showed that treatment with $30 \mu\text{g/mL}$ SPC resulted in the formation of larger myotubes, accompanied by a higher myoblast fusion index, which indicates the number of nuclei within MyHC-positive myotubes (Figure 2).

To determine whether the effects on myotube growth were specific to SPC, we compared it with soybean PC (Soy-PC), which is composed almost entirely of common diacyl-type PC. As shown in Figure 3a, SPC appeared to increase myotube size, whereas no significant changes were observed following Soy-PC treatment. Consistent with microscopic observations, PCR analysis showed a significant increase in the mRNA expression of *Myh1* and *Myh4* after SPC treatment. In contrast, *Myh* mRNA levels did not increase in cells treated with Soy-PC (Figure 3b).

SPC Analysis. The characteristic abundance of Alk-PC in echinoderms has been previously reported. Kostetsky et al.¹⁹ described that the major Alk-PC molecular species in starfish *Distolasterias nipon* and *Asterias amurensis* consist of C16 and C18 alkyl chains with EPA and AA, respectively. Consistent with previous studies,^{19,23} the fatty acid composition of SPC

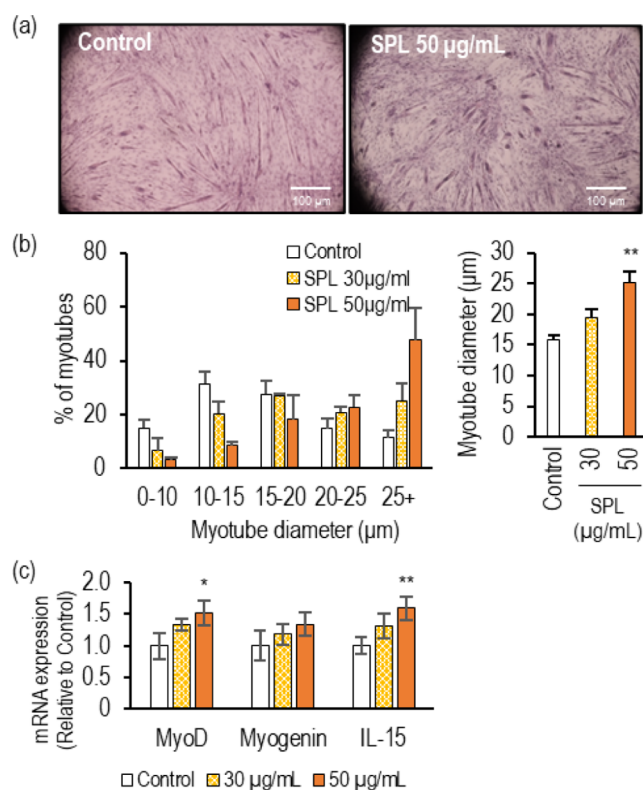


Figure 1. Effect of SPL on myotube formation in C2C12 cells. C2C12 myoblasts were induced to differentiate with starfish phospholipids (SPL) (0–50 $\mu\text{g/mL}$) and stained with HE on day 7 of differentiation. (a) Representative images of HE-stained myotubes. (b) Myotube diameter on day 7 of differentiation. (c) mRNA expression levels of MyoD, myogenin, and IL-15, measured using RT-PCR. Values are presented as mean \pm SD ($n = 3$). Statistical significance was determined using Dunnett's method, * $p < 0.05$.

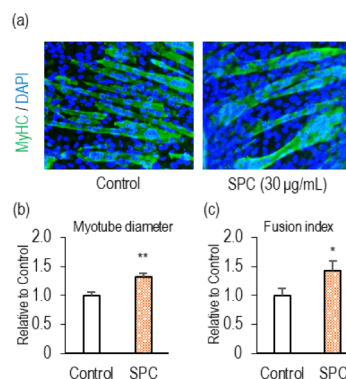


Figure 2. Immunostaining of myotubes with myosin heavy chain (MyHC) and analysis of myotube diameter and myoblast fusion index. C2C12 cells were induced to differentiate with or without SPC (30 $\mu\text{g/mL}$). (a) Representative immunofluorescence images of myotubes stained with MyHC (green) and DAPI (blue). (b) Myotube diameters relative to the control. (c) Myoblast fusion index, expressed as the percentage of fused myoblasts over total nuclei. Values are presented as mean \pm SD ($n = 3$). Statistical significance was determined using the Student's *t*-test, * $p < 0.05$.

showed that EPA and AA accounted for $28.8 \pm 0.5\%$ and $24.3 \pm 0.6\%$, respectively (Table 1). Additionally, long-chain monounsaturated fatty acids, including 20:1 and 18:1 fatty acids, was highly detected. Then, we separated the phospholipid subclasses using a method based on their

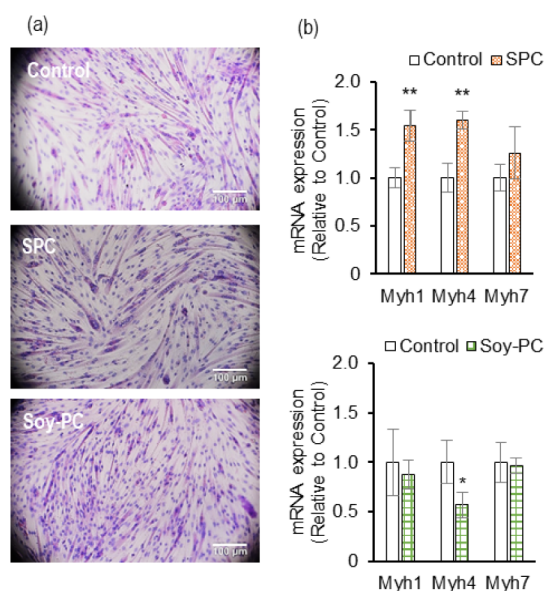


Figure 3. Comparison between SPC and soy-PC on C2C12 myotube formation. C2C12 cells were induced to differentiate in the presence or absence of SPC or soy-PC at 30 $\mu\text{g}/\text{mL}$. (a) Microscopic images of HE-stained myotubes. (b) RT-PCR analysis of MyHC mRNA expression. Values are presented as mean \pm SD ($n = 3$). Statistical significance was determined using the Student's *t*-test, * $p < 0.05$, ** $p < 0.01$.

Table 1. Fatty Acid Composition of SPC Fraction

Fatty acid	% (w/w)
16:0, palmitic acid	1.73 \pm 0.11
18:0, stearic acid	3.35 \pm 0.04
18:1n-9, oleic acid	1.52 \pm 0.02
18:1n-7	4.76 \pm 0.09
20:1n-9	6.59 \pm 0.54
20:1n-7	4.14 \pm 0.14
20:4n-6, AA	28.84 \pm 0.54
20:5n-3, EPA	24.26 \pm 0.61
22:6n-3, DHA	1.69 \pm 0.02
24:1n-9	1.46 \pm 0.01
others	21.65 \pm 0.81

different reactivities to hydrolysis by acids or bases against fatty acid esters, alkyl chains, and alkenyl chains bound to the glycerol backbone.²⁴ As shown in Figure 4a, Alk-PC accounted for more than 40% of the SPC.

The ESI spectra revealed a comprehensive profile of the ionized PC species present in the SPC (Figure 4). The spectra exhibited prominent molecular ion peaks in the range of m/z 790–800, including abundant peaks at m/z 792.8, 794.8, and 796.8. The LIPID MAPS database (<https://www.lipidmaps.org/>) suggests that Alk- and Pls-PC molecules with these masses are (O)38:6-, (P)38:5-, (O)38:5-, (P)38:4-, and (O)38:4-PC. We further conducted tandem MS analysis to identify the abundant PC molecular species. MS/MS analysis in positive multiple reaction monitoring (MRM) mode provided information on the structures of phosphocholine at *sn*-3 with the corresponding product ion at m/z 184. The chromatogram showing the precursor ion-to-product ion transitions at m/z 792.8 > 184, 794.8 > 184, and 796.8 > 184 revealed four abundant PC molecular species (Figure 4c).

To further verify the molecular structure, negative MRM mode was operated with transitions of the acetate adduct of precursor ion $[M + \text{CH}_3\text{COO}]^-$ to product deprotonated EPA and AA ($[\text{FA}-\text{H}]^-$) (Table S1). As shown in Figure 4c, the peaks of transition with product ions m/z 301.5 and 303.5, corresponding to EPA and AA, respectively, overlapped with the PC peaks. The abundant molecules present in SPC are suggested to bind AA or EPA with 18:0 or 18:1 alkyl or alkenyl chains (Table 2). The most prominent peak at m/z 794.8 was identified as (O)18:0/EPA-PC and (P)18:0/AA-PC, and the second-largest peak at m/z 796.8 was identified as (O)18:0/AA-PC.

Effect of EPA/AA-Binding Ether-Type PCs on C2C12 Myotube Formation. To determine the activities of ether-PC molecular species present in SPC, we compared their effects on myotube formation using diacyl-, alkyl-, and Pls-PCs (16:0/AA-, (O)16:0/AA-, (O)16:0/EPA-, and (P)16:0/AA-PC), which are commercially available. C2C12 cells treated with (O)16:0/EPA and (O)16:0/AA exhibited promoted myotube growth, with a significant increase in myotube diameter compared to the control group (Figure 5a,b). Treatment with (P)16:0/AA-PC showed a trend of increased myotube diameter at the concentration of 20 μM . In contrast, no difference was observed with the diacyl-type 16:0/AA-PC.

Additionally, there was a noticeable trend of increased mRNA expression of IL-15, which is one of the most abundant myokines expresses in myofibers, in cells treated with ether-type PC molecules (Figure 5c). This indicates distinct effects of diacyl and ether PCs on C2C12 myotube formation.

DISCUSSION

PUFA-binding PLs in cellular membranes play a pivotal role in modulating membrane fluidity and function. In both human and mouse skeletal muscle, phospholipids are primarily composed of approximately 50% PC and 25% PE, with smaller amounts of PS, phosphatidylinositol, and sphingomyelin.²⁵ Mouse skeletal muscle contains abundant PUFA-PC including 16:0/AA-PC and 16:0/DHA-PC.²⁶ Additionally, the quality of membrane phospholipids, defined by their fatty acid composition and molecular species, has been linked to muscle fiber type (slow-twitch/fast-twitch),²⁷ exercise training,^{28,29} and muscle diseases.^{30,31} These findings indicate that the cellular constituents of PC are closely associated with skeletal muscle function and homeostasis. However, our understanding of the functions of ether-type PC in muscle cells remains limited. In this study, we found for the first time that treatment with SPL enhanced myotube growth in C2C12 cells (Figure 1) and elucidated the contribution of the SPC, which comprises more than 50% ether-type PLs. Importantly, SPC treatment increased myotube size and mRNA levels of MyHC, whereas no changes were observed in cells treated with diacyl-type soybean PC (Figures 2 and 3). These results suggest that the specific activity of the PC molecular species contained in SPC is crucial for myotube growth and function.

Starfish commonly contain high levels of AA and EPA.²³ Kostetsky et al.¹⁹ investigated the PL composition at the molecular species level in six species of echinoderms, including the starfish *Distolasterias nipon* and *Asterias amurensis*. They found that the PC in these species contained approximately 65% Alk-PC, with (O)16:0/EPA-PC and (O)18:0/EPA-PC being the most prominent. In the present study, we determined that the SPC derived from *Patiria pectinifera* accounted for 41.4% Alk-PC and 7.2% Pls-PC (Figure 4a). LC-MS/MS

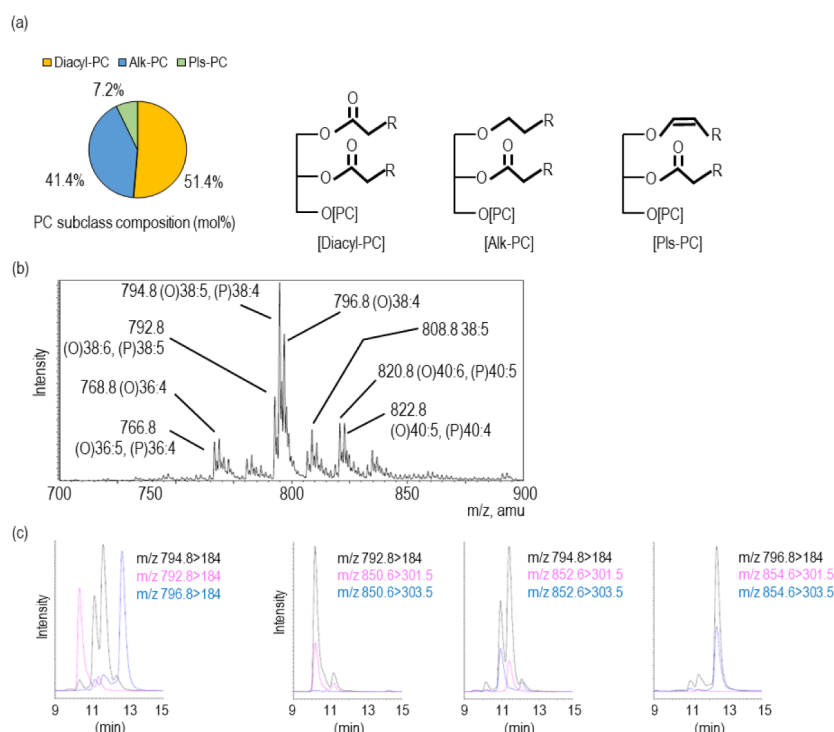


Figure 4. Analysis of the subclass composition and molecular species in starfish PC. (a) Structures and composition of PC subclasses in SPC measured using the Rouser method and HPLC-ELSD. (b) ESI+ MS spectrum of SPC, with “(O)” indicating alkylacyl and “(P)” indicating alkenylacyl. (c) Chromatogram showing the precursor ion ($[M + H]^+$) to product ion transitions m/z 794.8 > 184, 792.8 > 184, and 796.8 > 184, and chromatogram displaying the acetate-adducted parent ion ($[M + CH_3COO]^-$) transitioning to product ions with m/z 301.5 and 303.5 (ion intensity multiplied by 20). Retention times are indicated on the x -axis, and ion intensity is represented on the y -axis.

Table 2. Abundant PC Species in SPC Estimated by MRM Transitions

Mass	PC	Positive		Negative		Estimated species
		$[M+H]^+ > 184$		$[M+CH_3COO]^- > [FA-H]^-$		
		Q1	Q3	Q1	Q3	
791.6	(O)38:6	792.8	184	850.6	301.5	(O)18:1/EPA-PC
	(P)38:5				301.5	(P)18:0/EPA-PC
793.6	(O)38:5	794.8	184	852.6	301.5	(O)18:0/EPA-PC
	(P)38:4				303.5	(O)18:1/AA-PC
					303.5	(P)18:0/AA-PC
795.6	(O)38:4	796.8	184	854.6	303.5	(O)18:0/AA-PC

analysis revealed that the molecular species in SPC were predominantly ether-type PCs, including (O)38:4-PC and (O)38:5-PC. Additionally, MRM analysis successfully identified the binding of EPA or AA to PC molecules (Figure 4b,c). These results suggest that the prominent peaks at m/z 794.8 and 796.8 correspond to (O)18:0/EPA-PC and (O)18:0/AA-PC, respectively. Furthermore, the MS spectrum peaks at m/z 766.8, 768.8, 820.8, and 822.8 correspond to (O)36:4-PC, (O)36:5-PC, (O)40:4-PC, and (O)40:5-PC, respectively. These findings indicate the presence of Alk-PCs with C16 or C20 alkyl chains and EPA or AA.

Previous studies have shown the regulatory effects of various fatty acids on myoblast proliferation and differentiation.³² AA was found to enhance myotube growth in C2C12 cells through the cyclooxygenase-2-dependent production of prostaglandins E2 and F2.³³ In contrast, some research groups have reported

that supplemental free form EPA inhibits myogenesis and down-regulates the expression of muscle related genes in C2C12 cells.^{34,35} We also observed the inhibition of myotube formation in EPA treated C2C12 cells although significant effect of AA was not observed (Figure S1). These references and our results indicate that EPA and AA have a different effect on muscle differentiation. In the present study, on the other hand, we revealed that both Alk-PC species bound with AA and EPA increased myotube size (Figure 5a,b). In addition, Pls-type, but not diacyl-type, bound to AA promoted myotube growth. These results clearly showed that the effects differ depending on the PC form supplied, suggesting that the characteristic promotion of muscle differentiation and growth by SPC is due to the PC structure rather than the fatty acids. Furthermore, ether-PCs tended to increase the mRNA expression of the myokine Il-15 (Figure 5c), suggesting that they influence not only size but also muscle function. Hsueh et al.³⁴ have reported that EPA treatment induce adipogenesis during C2C12 differentiation. Interestingly, our results are the first to reveal that treatment with Alk-PC bound with EPA promotes C2C12 myotube growth (Figure 5). These different activities observed among free fatty acids, diacyl-PCs and ether-PCs underscore the structural importance of PCs with ether-bonded alkyl/alkenyl chains in regulating the C2C12 differentiation process.

While this study focused on evaluating the effects on myotube growth, the detailed mechanisms underlying these effects will need to be addressed in future research. Alk- and Pls-PLs play crucial roles in regulating membrane physicochemical properties, such as fluidity, fission, fusion, and morphological transitions.^{36,37} Previous studies have demonstrated that Pls-PLs promote membrane fusion processes.^{38,39}

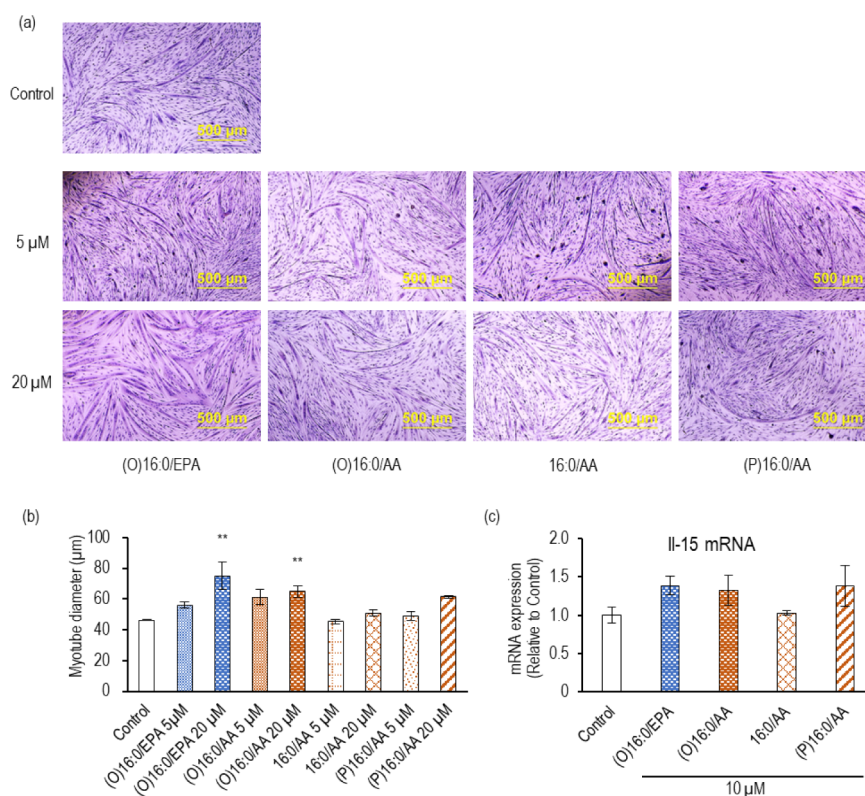


Figure 5. Effects of EPA/AA-binding ether-linked PC on C2C12 myotube formation. C2C12 cells were treated with (O)16:0/EPA-, (O)16:0/AA-, 16:0/AA-, or (P)16:0/AA-PC during differentiation at a concentration of 5, 10, or 20 μM . (a) Microscopic images of HE-stained myotubes. (b) Myotube diameter and (c) IL-15 mRNA expression on day 7 of differentiation. Values are presented as mean \pm SD ($n = 3$). Statistical significance was determined using Dunnett's method, * $p < 0.05$, ** $p < 0.01$

The structural and physical properties of starfish-derived ether PC may modulate the membrane environment and the dynamics of myoblast fusion during differentiation. Further analysis of the lipid class and molecular species composition of the cell membrane is required to confirm their PL function. Additionally, the effects of other ether subclasses of PL, such as PE, need to be evaluated. Understanding the influence of the ether structure on myoblast fusion and myotube growth signaling is also important in nutritional approach.

In conclusion, we identified Alk- and Pls-PC with EPA or AA in SPL as active compounds for promoting C2C12 myotube growth. Our findings highlight the novel functionality of SPC and provide valuable insights into the functional properties of PLs with alkyl and alkenyl chains in muscle function. Consequently, our study demonstrates the potential utility of SPL as a functional food and nutraceutical agent for improving muscle health in human.

MATERIALS AND METHODS

Materials. The starfish *Patiria pectinifera*, commonly found in the northern Pacific Ocean along the coasts of Japan, China, and Russia, was generously provided by the Hakodate Fishery Cooperative (Hokkaido, Japan). Soy-PC (1- α -phosphatidylcholine) was obtained from Avanti Polar Lipids (Alabaster, AL, USA). The following PC were purchased from Cayman Chemical Co. (Ann Arbor, MI, USA): 1-palmitoyl-2-arachidonoyl-*sn*-glycero-3-PC (16:0/AA-PC), 1-*O*-hexadecyl-2-arachidonoyl-*sn*-glycero-3-PC ((O)16:0/AA-PC), 1-*O*-hexadecyl-2-eicosapentaenoyl-*sn*-glycero-3-PC ((O)16:0/EPA-PC), and 1-1(*Z*)-hexadecenyl-2-arachidonoyl-*sn*-glycero-3-PC

((P)16:0/AA-PC). All organic solvents were purchased from FUJIFILM Wako Pure Chemicals (Osaka, Japan).

Sample Preparation. Total lipids were extracted from the starfish as described in a previous study.²² These lipids were then divided into three main fractions: neutral lipids, glycolipids, and SPL, using silica gel chromatography and elution with chloroform, acetone, and methanol, respectively. The SPL fraction was further classified using preparative thin layer chromatography (PLC Silica gel 60 F254, 1 mm, Merck KGaA, Darmstadt, Germany), developed with a chloroform/methanol/water mixture (25:15:2, v/v/v). The R_f values of each PL class were compared with standards and PE, PS, PC and LPC were identified in the SPL. Each fraction was extracted from the silica gel using a chloroform/methanol mixture (1:1, v/v), and the lipid class composition was determined by weight percentage.

Lipid Analysis. The fatty acids in the SPC were converted into methyl ester derivatives as described by Prevot and Mordret.⁴⁰ The fatty acid composition was analyzed using a gas chromatograph (GC-2014; Shimadzu Corporation, Kyoto, Japan) equipped with a flame ionization detector. The fatty acids were identified based on the retention times of a standard fatty acid methyl ester solution (Supelco 37 Component FAME Mix; Merck KGaA, Darmstadt, Germany).

The composition of the PC subclass was determined using the methods described by Dawson.²⁴ Briefly, fractionated SPC was subjected to hydrolysis using a 0.5 N KOH-ethanol solution at 70 $^{\circ}\text{C}$ for 30 min. The reaction mixture was then separated into water and chloroform phases, with glycerophosphocholine derived from diacyl-PC collected in the aqueous layer (A). A 2 N HCl-methanol solution was added to

the chloroform layer (B), containing lysoalkenyl-PC and lysoalkyl-PC originating from Pls- and Alk-PC, respectively. In the reaction at 75 °C for 2 h, lysoalkenyl-PC was subjected to acid-hydrolysis, yielding glycerophosphocholine that was partitioned into the aqueous layer (C). The phosphorus content of each fraction was quantified using the Rauser method.⁴¹ The composition ratio of each subclass was calculated as follows: diacyl-PC:Pls-PC:Alk-PC = A:C:(B–C), and the results are expressed in mol %.

Qualitative analysis of SPC molecular species was performed using an HPLC–MS/MS system equipped with a Shimadzu MS-8040 mass spectrometer (Kyoto, Japan) and an electrospray ionization source. Gradient chromatographic separation was performed on a Kinetex C18 core–shell column (2.1 × 100 mm, 2.6 μm, Phenomenex Inc., Torrance, CA, USA) at a flow rate of 0.3 mL/min. The mobile phase consisted of (A) acetonitrile:methanol:water (1:1:3, v/v/v) with 5 mM ammonium acetate and (B) isopropanol with 5 mM ammonium acetate. The gradient elution was as follows: 0–1 min, 0% B; 1–5 min, a linear gradient to 40% B; 5–7 min, an increase to 64% B; 7–12 min, held at 64% B; 12–12.5 min, a step to 82.5% B; 12.5–19 min, an increase to 85% B; 19–20 min, an increase to 95% B; 20–25 min, held at 95% B; 25.1–30 min, re-equilibration to 0% B. Among the numerous molecules, a total of 18 PC molecular species binding either EPA or AA were identified via LC–MS/MS operating in the MRM mode (Table S1). A heated electrospray ionization source was used in both positive and negative modes. MS conditions were as follows: interface voltage, 2500 V; nebulizer gas (Ar), 2 L/min; drying gas (N₂), 15 L/min; heating block temperature, 400 °C; CID gas, 230 kPa.

Cell Culture. Mouse C2C12 myoblasts were obtained from the American Type Culture Collection (Manassas, VA, USA) and cultured in Dulbecco's modified Eagle's medium (DMEM) containing 10% (v/v) calf serum (CS) and supplemented with 1% (v/v) penicillin-streptomycin solution (FUJIFILM Wako Pure Chemicals). The cells were maintained in 5% CO₂ at 37 °C. The C2C12 myoblasts were seeded onto a collagen-coated microplate (IWAKI AGC Techno Glass Co., Ltd., Shizuoka, Japan). Once the cells reached confluence, myogenic differentiation was initiated using differentiation medium (DM), which is DMEM containing 2% (v/v) horse serum (day 0). Differentiation continued until day 7, with the medium being changed every 2 days. The lipid samples were added as an ethanol solution to the DM (<0.1% ethanol), while control cells received the same amount of vehicle ethanol.

Morphological Analysis. Myotube formation was observed using hematoxylin and eosin (HE) staining. To analyze morphological changes, five images from different fields of view were randomly taken from each well. The thickness of the 10 myotubes with the largest diameters in each image was measured using ImageJ software (National Institutes of Health). Total of 50 myotubes were analyzed with three biological replicates per group.

To measure the myotube fusion index, C2C12 myoblasts were seeded on coverslips coated with polyethylenimine in 6-well plates, and myogenic differentiation was induced as described above. At the indicated times, cells were fixed with 100% cold methanol, blocked with 1% bovine serum albumin in PBS, and incubated with MyHC monoclonal antibody (Clone MF20, R&D Systems, Inc., Minneapolis, MN, USA) at 10 μg/mL. This was followed by incubation with the

secondary antibody, Alexa Fluor 488-conjugated antirabbit IgG (Proteintech Group, Inc., Rosemont, IL, USA). Nuclei were stained with 4',6'-diamidino-2-phenylindole (DAPI), and the cells were covered with coverslips for microscopic observation. The myotube fusion index was measured as the ratio of the number of nuclei in MyHC-positive myotubes to the total number of nuclei in the field.

Polymerase Chain Reaction (PCR) Assay. Total RNA was extracted from C2C12 myotubes using QIAzol lysis reagent (Qiagen, Hilden, Germany) according to the manufacturer's protocol. The extracted RNA was then reverse transcribed into cDNA using the High-Capacity cDNA Archive Kit (Applied Biosystems Japan Ltd., Tokyo, Japan). Reverse transcription quantitative PCR (RT-qPCR) was performed with a StepOnePlus real-time PCR system (Applied Biosystems Japan Ltd.). For the PCR reaction, GeneAce Probe qPCR Mix (Nippon Gene, Tokyo, Japan) was utilized, and the cycling conditions were as follows: 50 °C for 2 min, 95 °C for 10 min, followed by 40 cycles of 95 °C for 30 s and 60 °C for 1 min.

mRNA expression levels were measured using TaqMan Gene Expression Assays (Thermo Fisher Scientific, Frederick, MD, USA) with the following probes: Il-15, Mm00434210_m1; MyoD, Mm00440387_m1; Myogenin, Mm00446194_m1; Myh1, Mm01332489_m1; Myh4, Mm01332541_m1; Myh7, Mm00600555_m1; and Rn18s, Mm04277571_s1. Expression levels were normalized using Rn18s as an internal standard.

Statistical Analysis. Data are expressed as mean ± SD (*n* = 3). Significant differences were analyzed using the Student's *t*-test or one-way analysis of variance, followed by posthoc Dunnett's tests for pairwise comparisons with the control group.

■ ASSOCIATED CONTENT

Supporting Information

The Supporting Information is available free of charge at <https://pubs.acs.org/doi/10.1021/acsomega.4c07865>.

Microscopic images of C2C12 cells treated with/without EPA or AA during differentiation, and LC–MS/MS MRM transition of PC molecules containing either EPA or AA (PDF)

■ AUTHOR INFORMATION

Corresponding Author

Fumiaki Beppu – Faculty of Fisheries Sciences, Hokkaido University, Hakodate, Hokkaido 041-8611, Japan;
orcid.org/0000-0002-1730-3740; Phone: +81-138-40-8804; Email: fbeppu@fish.hokudai.ac.jp

Authors

Aoi Fukushima – Faculty of Fisheries Sciences, Hokkaido University, Hakodate, Hokkaido 041-8611, Japan
Kiyosuke Imamura – Faculty of Fisheries Sciences, Hokkaido University, Hakodate, Hokkaido 041-8611, Japan
Naoki Takatani – Faculty of Fisheries Sciences, Hokkaido University, Hakodate, Hokkaido 041-8611, Japan
Masashi Hosokawa – Faculty of Fisheries Sciences, Hokkaido University, Hakodate, Hokkaido 041-8611, Japan;
orcid.org/0000-0003-1755-3173

Complete contact information is available at:
<https://pubs.acs.org/doi/10.1021/acsomega.4c07865>

Author Contributions

A.F. contributed to conceptualization, methodology, investigation, formal analysis, and writing-review and editing. K.I. contributed to investigation, validation, formal analysis, and writing-review and editing. N.T. contributed to conceptualization, methodology, and writing-review and editing. M.H. contributed to conceptualization, methodology, funding, writing-review and editing, and supervision. F.B. contributed to conceptualization, methodology, formal analysis, funding, writing-original draft, visualization, supervision, and project administration.

Notes

The authors declare no competing financial interest.

ACKNOWLEDGMENTS

This work was supported by Foundation, Oil & Fat Industry Kaikan, Lotte Research Promotion Grant and by grants from Japan Society for the Promotion of Science KAKENHI (20K06221). We would like to thank Editage (www.editage.jp) for English language editing.

REFERENCES

- (1) Metter, E. J.; Talbot, L. A.; Schrager, M.; Conwit, R. Skeletal muscle strength as a predictor of all-cause mortality in healthy men. *J. Gerontol., Ser. A* **2002**, *57* (10), B359–65.
- (2) Heitmann, B. L.; Frederiksen, P. Thigh circumference and risk of heart disease and premature death: Prospective cohort study. *BMJ* **2009**, *339*, b3292.
- (3) Rantanen, T.; Harris, T.; Leveille, S. G.; Visser, M.; Foley, D.; Masaki, K.; Guralnik, J. M. Muscle strength and body mass index as long-term predictors of mortality in initially healthy men. *J. Gerontol., Ser. A* **2000**, *55* (3), M168–73.
- (4) Donini, L. M.; Busetto, L.; Bischoff, S. C.; Cederholm, T.; Ballesteros-Pomar, M. D.; Batsis, J. A.; Bauer, J. M.; Boirie, Y.; Cruz-Jentoft, A. J.; Dicker, D.; Frara, S.; Frühbeck, G.; Genton, L.; Gepner, Y.; Giustina, A.; Gonzalez, M. C.; Han, H. S.; Heymsfield, S. B.; Higashiguchi, T.; Laviano, A.; Lenzi, A.; Nyulasi, I.; Parrinello, E.; Poggiogalle, E.; Prado, C. M.; Salvador, J.; Rolland, Y.; Santini, F.; Serlie, M. J.; Shi, H.; Sieber, C. C.; Siervo, M.; Vettor, R.; Villareal, D. T.; Volkert, D.; Yu, J.; Zamboni, M.; Barazzoni, R. Definition and diagnostic criteria for sarcopenic obesity: ESPEN and EASO consensus statement. *Clin. Nutr.* **2022**, *41* (4), 990–1000.
- (5) Wang, M.; Tan, Y.; Shi, Y.; Wang, X.; Liao, Z.; Wei, P. Diabetes and Sarcopenic Obesity: Pathogenesis, Diagnosis, and Treatments. *Front. Endocrinol.* **2020**, *11*, 568.
- (6) Shen, Y.; Zhang, C.; Dai, C.; Zhang, Y.; Wang, K.; Gao, Z.; Chen, X.; Yang, X.; Sun, H.; Yao, X.; et al. Nutritional Strategies for Muscle Atrophy: Current Evidence and Underlying Mechanisms. *Mol. Nutr. Food Res.* **2024**, *68*, No. e2300347.
- (7) Liu, S.; Zhang, L.; Li, S. Advances in nutritional supplementation for sarcopenia management. *Front. Nutr.* **2023**, *10*, 1189522.
- (8) Schuchardt, J. P.; Hahn, A. Bioavailability of long-chain omega-3 fatty acids. *Prostaglandins, Leukotrienes Essent. Fatty Acids* **2013**, *89* (1), 1–8.
- (9) Ulven, S. M.; Kirkhus, B.; Lamglait, A.; Basu, S.; Elind, E.; Haider, T.; Berge, K.; Vik, H.; Pedersen, J. I. Metabolic effects of krill oil are essentially similar to those of fish oil but at lower dose of EPA and DHA, in healthy volunteers. *Lipids* **2011**, *46* (1), 37–46.
- (10) Rossmeisl, M.; Jilkova, Z. M.; Kuda, O.; Jelenik, T.; Medrikova, D.; Stankova, B.; Kristinsson, B.; Haraldsson, G. G.; Svendsen, H.; Stoknes, I.; et al. Metabolic effects of n-3 PUFA as phospholipids are superior to triglycerides in mice fed a high-fat diet: Possible role of endocannabinoids. *PLoS One* **2012**, *7* (6), No. e38834.
- (11) Hosokawa, M.; Sato, A.; Ishigamori, H.; Kohno, H.; Tanaka, T.; Takahashi, K. Synergistic effects of highly unsaturated fatty acid-containing phosphatidyl-ethanolamine on differentiation of human

leukemia HL-60 cells by dibutyl cyclic adenosine monophosphate. *Jpn. J. Cancer Res.* **2001**, *92* (6), 666–672.

- (12) Ishigamori, H.; Hosokawa, M.; Kohno, H.; Tanaka, T.; Miyashita, K.; Takahashi, K. Docosahexaenoic acid-containing phosphatidylethanolamine enhances HL-60 cell differentiation by regulation of c-jun and c-myc expression. *Mol. Cell. Biochem.* **2005**, *275* (1–2), 127–133.

- (13) Dean, J. M.; Lodhi, I. J. Structural and functional roles of ether lipids. *Protein Cell* **2018**, *9* (2), 196–206.

- (14) Nishimukai, M.; Wakisaka, T.; Hara, H. Ingestion of plasmalogen markedly increased plasmalogen levels of blood plasma in rats. *Lipids* **2003**, *38* (12), 1227–1235.

- (15) Wang, X.; Chen, Q.; Wang, X.; Cong, P.; Xu, J.; Xue, C. Lipidomics Approach in High-Fat-Diet-Induced Atherosclerosis Dyslipidemia Hamsters: Alleviation Using Ether-Phospholipids in Sea Urchin. *J. Agric. Food Chem.* **2021**, *69* (32), 9167–9177.

- (16) Wang, X.; Wang, X.; Cong, P.; Wu, L.; Ma, Y.; Wang, Z.; Jiang, T.; Xu, J. Sea cucumber ether-phospholipids improve hepatic steatosis and enhance hypothalamic autophagy in high-fat diet-fed mice. *J. Nutr. Biochem.* **2022**, *106*, 109032.

- (17) Gomes, R.; Freitas, A.; Rocha-Santos, T.; Duarte, A. Bioactive compounds derived from echinoderms. *RSC Adv.* **2014**, *4*, 29365–29382.

- (18) Xia, J. -M.; Miao, Z.; Xie, C. -L.; Zhang, J. -W.; Yang, X. -W. Chemical Constituents and Bioactivities of Starfishes: An Update. *Chem. Biodiversity* **2020**, *17* (1), No. e1900638.

- (19) Kostetsky, E. Y.; Sanina, N. M.; Velansky, P. V. The thermotropic behavior and major molecular species composition of the phospholipids of echinoderms. *Russ. J. Mar. Biol.* **2014**, *40* (2), 131–139.

- (20) Dong, G.; Xu, T.; Yang, B.; Lin, X.; Zhou, X.; Yang, X.; Liu, Y. Chemical Constituents and Bioactivities of Starfish. *Chem. Biodiversity* **2011**, *8*, 740–791.

- (21) Yamagishi, M.; Hosoda-Yabe, R.; Tamai, H.; Konishi, M.; Imamura, A.; Ishida, H.; Yabe, T.; Ando, H.; Kiso, M. Structure-Activity Relationship Study of the Neuritogenic Potential of the Glycan of Starfish Ganglioside LLG-3 (±). *Mar. Drugs* **2015**, *13* (12), 7250–7274.

- (22) Beppu, F.; Li, H.; Yoshinaga, K.; Nagai, T.; Yoshinda, A.; Kubo, A.; Kanda, J.; Gotoh, N. Dietary Starfish Oil Prevents Hepatic Steatosis and Hyperlipidemia in C57BL/6N Mice Fed High-fat Diet. *J. Oleo Sci.* **2017**, *66* (7), 761–769.

- (23) Howell, K.; Pond, D.; Billett, T. Feeding ecology of deep-sea seastars (Echinodermata: Asteroidea): A fatty-acid biomarker approach. *Mar. Ecol.: Prog. Ser.* **2003**, *255*, 193–206.

- (24) Dawson, R. M. A hydrolytic procedure for the identification and estimation of individual phospholipids in biological samples. *Biochem. J.* **1960**, *75* (1), 45–53.

- (25) Simon, G.; Rouser, G. Species variations in phospholipid class distribution of organs. II. Heart and skeletal muscle. *Lipids* **1969**, *4* (6), 607–614.

- (26) Cortie, C. H.; Hulbert, A. J.; Hancock, S. E.; Mitchell, T. W.; McAndrew, D.; Else, P. L. Of mice, pigs and humans: An analysis of mitochondrial phospholipids from mammals with very different maximal lifespans. *Exp. Gerontol.* **2015**, *70*, 135–143.

- (27) Janovská, A.; Hatzinikolas, G.; Mano, M.; Wittert, G. A. The effect of dietary fat content on phospholipid fatty acid profile is muscle fiber type dependent. *Am. J. Physiol. Endocrinol. Metab.* **2010**, *298* (4), No. E779–86.

- (28) Andersson, A.; Sjödin, A.; Olsson, R.; Vessby, B. Effects of physical exercise on phospholipid fatty acid composition in skeletal muscle. *Am. J. Physiol.* **1998**, *274* (3), No. E432–8.

- (29) Goto-Inoue, N.; Yamada, K.; Inagaki, A.; Furuichi, Y.; Ogino, S.; Manabe, Y.; Setou, M.; Fujii, N. L. Lipidomics analysis revealed the phospholipid compositional changes in muscle by chronic exercise and high-fat diet. *Sci. Rep.* **2013**, *3*, 3267.

- (30) Senoo, N.; Miyoshi, N.; Kobayashi, E.; Morita, A.; Tanihata, J.; Takeda, S.; Miura, S. Glycerophospholipid profile alterations are

associated with murine muscle-wasting phenotype. *Muscle Nerve* **2020**, *62* (3), 413–418.

(31) Tuazon, M. A.; Henderson, G. C. Fatty acid profile of skeletal muscle phospholipid is altered in mdx mice and is predictive of disease markers. *Metabolism* **2012**, *61* (6), 801–811.

(32) Hurley, M. S.; Flux, C.; Salter, A. M.; Brameld, J. M. Effects of fatty acids on skeletal muscle cell differentiation in vitro. *Br. J. Nutr.* **2006**, *95* (3), 623–630.

(33) Markworth, J. F.; Cameron-Smith, D. Arachidonic acid supplementation enhances in vitro skeletal muscle cell growth via a COX-2-dependent pathway. *Am. J. Physiol. Cell Physiol.* **2013**, *304* (1), C56–67.

(34) Hsueh, T. Y.; Baum, J. I.; Huang, Y. Effect of Eicosapentaenoic Acid and Docosahexaenoic Acid on Myogenesis and Mitochondrial Biosynthesis during Murine Skeletal Muscle Cell Differentiation. *Front. Nutr.* **2018**, *5*, 15.

(35) Zhang, J.; Xu, X.; Liu, Y.; Zhang, L.; Odle, J.; Lin, X.; Zhu, H.; Wang, X.; Liu, Y. EPA and DHA Inhibit Myogenesis and Downregulate the Expression of Muscle-related Genes in C2C12 Myoblasts. *Genes* **2019**, *10*, 64.

(36) Koivuniemi, A. The biophysical properties of plasmalogens originating from their unique molecular architecture. *FEBS Lett.* **2017**, *591* (18), 2700–2713.

(37) Almshergji, Z. A. Potential Role of Plasmalogens in the Modulation of Biomembrane Morphology. *Front. Cell Dev. Biol.* **2021**, *9*, 673917.

(38) Glaser, P. E.; Gross, R. W. Plasmenylethanolamine facilitates rapid membrane fusion: A stopped-flow kinetic investigation correlating the propensity of a major plasma membrane constituent to adopt an HII phase with its ability to promote membrane fusion. *Biochemistry* **1994**, *33* (19), 5805–5812.

(39) Han, X. L.; Gross, R. W. Plasmenylcholine and phosphatidylcholine membrane bilayers possess distinct conformational motifs. *Biochemistry* **1990**, *29* (20), 4992–4996.

(40) Prevot, A. F.; Mordret, F. X. Use of glass capillary columns in gas chromatography for the analysis of fats. *Rev. Fr. Corps Gras* **1976**, *23*, 409–423.

(41) Rouser, G.; Fleischer, S.; Yamamoto, A. Two dimensional thin layer chromatographic separation of polar lipids and determination of phospholipids by phosphorus analysis of spots. *Lipids* **1970**, *5* (5), 494–496.